ARIEL VI MEASUREMENTS OF ULTRA-HEAVY COSMIC RAY FLUXES IN THE REGION $34 \leq Z \leq 48$

P.H. Fowler, M.R.W. Masheder, R.T. Moses,
R.N.F. Walker, A. Worley and A.M. Gay
H.H. Wills Physics Laboratory, University of Bristol,
Tyndall Avenue, Bristol BS8 1TL, England.

1. Introduction. The Ariel VI satellite was launched by NASA on a Scout rocket on 3rd June 1979 from Wallops Island, Virginia, USA, into a near-circular 625 km orbit inclined at 55°. It carried a spherical cosmic ray detector designed by a group from Bristol University. The salient features of this detector are shown in Fig. 1.

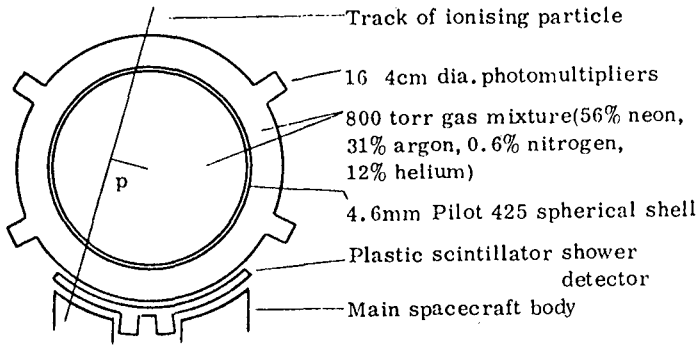

Fig. 1 Schematic cross-section of Ariel VI Cosmic ray detector

A spherical aluminium vessel of diameter 75 cm contains a gas scintillation mixture and a thin spherical shell of Pilot 425 plastic, and forms a single optical cavity viewed by 16 photomultipliers. Particle tracks through the detector may be characterised by their impact parameter p and by whether or not they pass through the cup of plastic scintillator placed between the sphere and the spacecraft body (referred to below as the Anti-Coincidence Detector or ACD). Individual particle charges are determined by separately measuring the gas scintillation and the Cerenkov emission from the plastic shell. This is possible because of the quite different distribution in time of these emissions. See also (1).

The last data from Ariel VI was received in February 1982, but spacecraft power supply problems had restricted data collection to only 427 of the days in orbit, with actual experiment live-time equivalent to 352 complete days at 100% efficiency.

2. Data Selection. Results from a first analysis of part of the Ariel VI data set have already been reported (2). The present analysis covers all available high charge data collected by Ariel VI. It includes improvements to the cut-off map used to apply cut-off labels to individual events and new event timings which allow for imperfections in the spacecraft clock by using measured cosmic ray fluxes as clock calibrations. Event timing, and the subsequent allocation of an inferred local vertical cut-off to an individual event, is important for the Ariel VI data analysis because a small number of low energy iron nuclei, which can stop in the detector at

high impact parameters, can simulate higher charges up to a limit of apparent charge 47. Hence, for abundance measurements in the charge region $34 \leq Z \leq 48$, data can only be accepted from those regions where the earth's magnetic field excludes such low energy iron nuclei. This is empirically determined to be for vertical cut-offs greater than 3.4 GV.

Finally, with the improved statistics from the complete mission, it is seen that events which produce a signal in the ACD (hits) have a cut-off distribution indicative of pollution from electron showers to the highest charges, though hardly statistically significant for $Z \geq 70$. The hit spectrum also shows evidence of additional fragmentation due to passage through the body of the spacecraft. Consequently these ACD hits require separate analysis and are not included in the results quoted in this paper or in the companion paper OG4.4-4.

3. Results. Fig. 2 shows the distribution of accepted data for this charge region. Numbers given are actual numbers of detected events, with two provisos: i) a correction has been made for the exponential tail associated with the relativistic rise in energy loss for charges 30,31,32 using measured abundances from HEAO3-C2 (3); this affects the first five bins: ii) some events in the lower part of this charge region have been collected as events of second highest priority (1), at lower efficiency, and in this case scaling has been made event by event to an equivalent 100% efficiency; this effect has become small by bin 8 onwards.

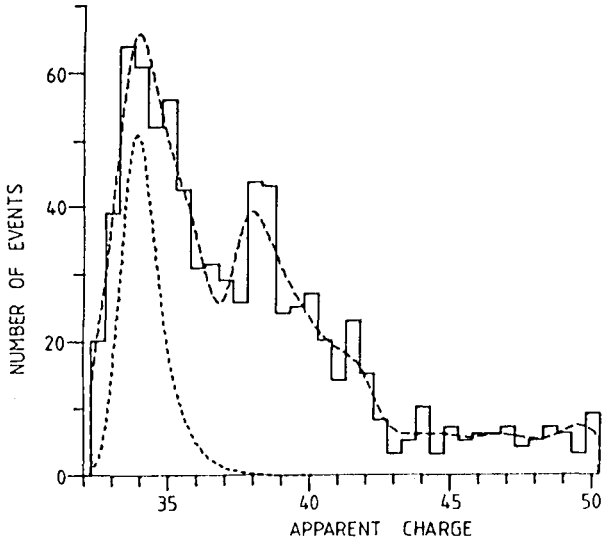

Fig. 2 Distribution of accepted data for determination of $33 \leq Z \leq 48$ abundances. Dotted insert shows distribution of $_{34}Se$ content from Table 1.

During data re-analysis small improvements have been made to charge allocation as a function of gain setting and an energy dependent non-Z^2 correction has been applied to all data. This is discussed further in OG4.4-4. Its effects are in any case small for $Z \leq 48$.

In order to allot events to individual charge species the effects of the resolution function of the experiment must be removed from the data in a deconvolution procedure. The resolution function is well determined

Table 1 Elemental Abundances for $33 \leq Z \leq 48$

Z	Ariel VI: Deconvolved Numbers	Ariel VI: Corrected to outside expt	Ariel VI: Charge pairs	Comparison Data: HEAO3-C3	Comparison Data: SS + FIPD propagations: Brewster et al.	Comparison Data: SS + FIPD propagations: Letaw et al.
	3.46×10^6	10^6	10^6		10^6	10^6
33	(81 ± 21)	(21 ± 6)	72 ± 5	[9]<19	11	68
34	180 ± 29	51 ± 8		43^{+10}_{-6}	55	
35	84 ± 25	24 ± 7	43 ± 4	[7]<14	10	31
36	71 ± 23	19 ± 6		23^{+8}_{-5}	24	
37	22 ± 20	6 ± 5	38 ± 4	[9]<16	20	47
38	110 ± 24	32 ± 7		35^{+10}_{-6}	46	
39	54 ± 25	14 ± 7	26 ± 4	[5]<12	8	24
40	42 ± 20	12 ± 6		13^{+5}_{-4}	16	
41	33 ± 22	9 ± 6	19 ± 4	[3]< 6	2.5	10
42	35 ± 13	10 ± 4		8 ± 2	6.5	
43	0		3 ± 2			7.0
44	12 ± 8					
45	13 ± 14		6 ± 2			6.0
46	9 ± 12					
47	14 ± 13		6 ± 2			4.9
48	9 ± 13					

for $_{26}Fe$ and is found to fit well to a Gaussian part and an exponential tail to high charge (2). In addition the shapes of the abundance peaks at $_{12}Mg$, $_{14}Si$ and $_{20}Ca$ allow the variance of the Gaussian to be separated into a Poisson part and a part varying as Z^2. A resolution function may then be constructed for any higher charge by extrapolation. The resolution function for $_{34}Se$ is shown as a dotted insert in Fig. 2. Using these functions the observed data may be deconvolved into a best-fit set of abundances, giving the numbers shown in column 2 of Table 1. These numbers yield the curve shown in Fig. 2 when operated on by the appropriate resolution functions. The fit is seen to be reasonably good, though the $Z = 38$ peak appears offset. The decrease in numbers of detected events around $Z = 43$ is too steep for the measured resolution function of the experiment. This fluctuation results in a best-fit abundance for $Z = 43$ which is approximately 1½ s.d. below zero. This value was set at zero and not varied in subsequent fitting procedures.

4. Discussion. The limited charge resolution achieved by the Ariel VI detector reveals only one clear charge peak in this region, at $Z = 38$, and only one odd charge, $Z = 35$, is strictly necessary to obtain a good fit to the data. Nevertheless the best-fit abundances in column 3, which have been corrected for fragmentation in the experiment, form the most convenient comparison with other work. The errors shown are the excur-

sions needed in a given abundance to produce a change of one unit of χ^2, the two neighbouring abundances being adjusted to keep the total area constant. They may be regarded as approximations to 1 s.d. errors for individual charges. With this procedure, fluctuations are strongly anti-correlated between neighbouring abundances and a significant decrease in the errors results when abundances for charge pairs are constructed as in column 4.

The best-fit values and upper limits presented by the HEAO3-C3 group at Bangalore (4) are shown in column 5, and agreement between the two experiments for individual charges is seen to be uniformly good, though the integrated total is rather higher for the Ariel VI data. Columns 6 and 7 of the table quote results from two propagations of Cameron (1982) solar system abundances (5) through about 6 $gmcm^{-2}$ of ISM with slightly different assumed First Ionisation Potential Dependence (Brewster et al. (6) and Letaw et al. (7)). Agreement between observed cosmic ray abundances and propagated SS is seen to be reasonably good in this area, with the FIPD of ref. (7), which saturates at potentials less than 7 eV, producing better agreement around charge 38.

5. Acknowledgements. The Ariel VI project has been supported throughout its lifetime by the UK Science and Engineering Research Council. A team from the Appleton Laboratory was responsible for project management and raw data handling when in orbit. Main spacecraft contractor was MSDS, Portsmouth. The Bristol experiment was built partially by support personnel within the Bristol Physics Department and partially by British Aerospace, Filton. The electronics for the Bristol experiment was built by Pye Telecommunications Ltd., Cambridge. We are indebted to all of the above for a successful mission.

6. References.

1. P.H. Fowler et al., 1979, Proc. 16th ICRC, Kyoto, 12, 338
2. P.H. Fowler et al., 1981, Nature, 291, 45
3. B. Byrnak et al., 1983, Proc. 18th ICRC, Bangalore, 2, 29
4. W.R. Binns et al., 1983, Proc. 18th ICRC, Bangalore, OG1-16
5. A.G.W. Cameron, 1982, in "Essays in Nuclear Astrophysics" ed. C.A. Barnes et al.
6. N.R. Brewster et al., 1983, Ap. J. 264, 324
7. J.R. Letaw et al., 1984, Ap. J. 279, 144